nature geoscience

Supplementary information

https://doi.org/10.1038/s41561-026-02050-w

European summer drying largely driven by atmospheric circulation changes since the 1980s

In the format provided by the authors and unedited

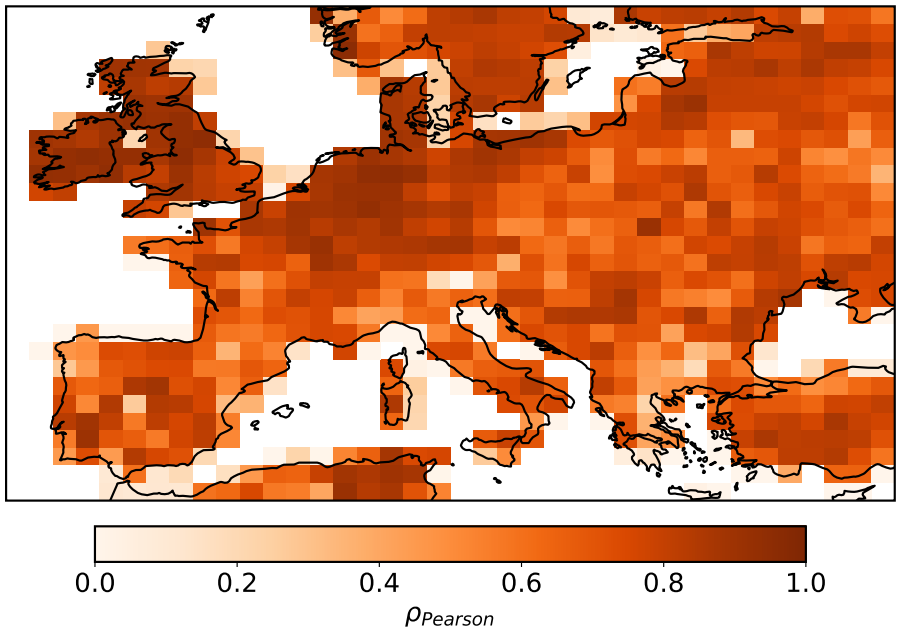

Supplementary Figure 1. Performance evaluation of CESM2 nudged circulation simulations. Pearson Correlation between summer 10 cm soil moisture anomalies in HIST and ERA5 (7 cm) in the period 2015 to 2023. Basemap is generated with cartopy.

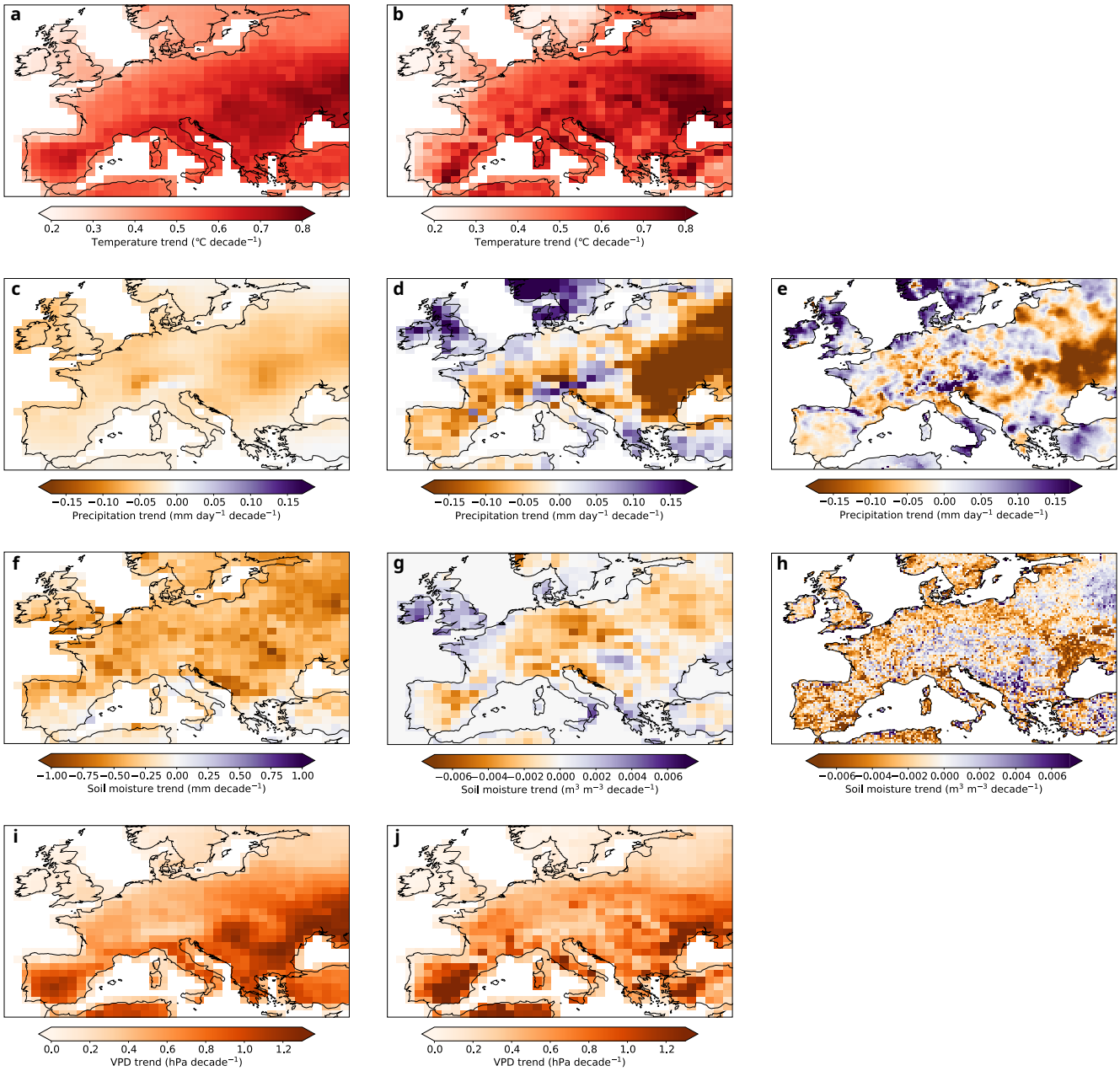

Supplementary Figure 2. Trends of summer hydroclimatic variables for the period 1980 – 2024. *a temperature in the CESM2 large ensemble (LENS2), b temperature in ERA5, c precipitation in LENS2, d precipitation in ERA5, e precipitation in E-OBS, f soil moisture in LENS2, g soil moisture in the first soil layer of ERA5, h soil moisture in ESA-CCISM, i VPD in LENS2, and j vapour pressure deficit (VPD) in ERA5. Basemaps are generated with cartopy.*

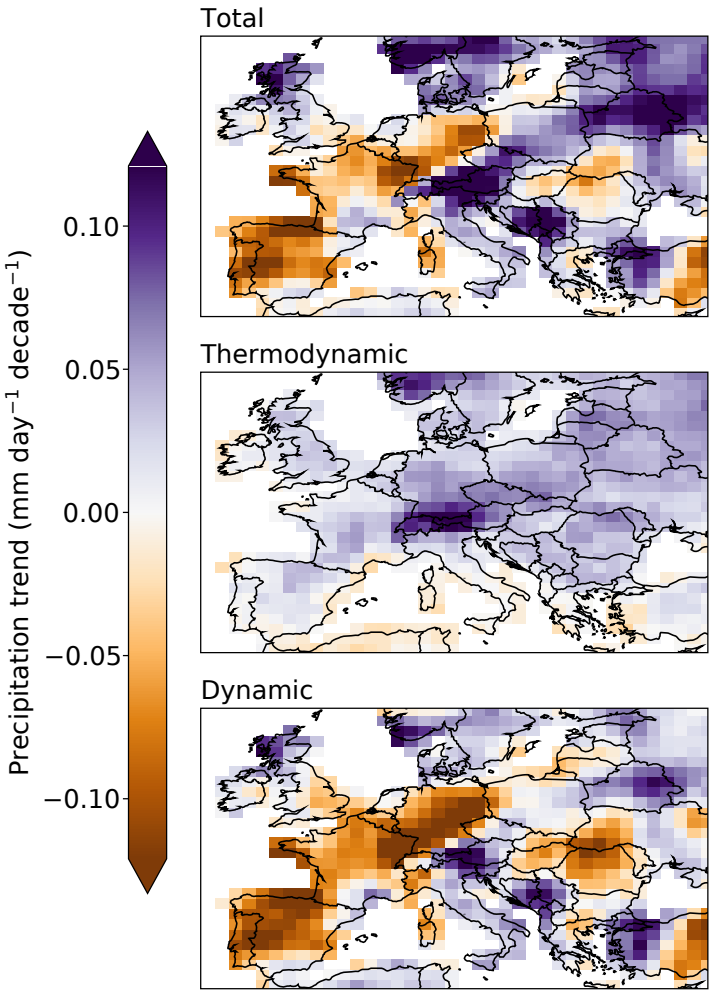

Supplementary Figure 3. Multi-decadal dynamic and thermodynamic precipitation trend in April and May over Europe. Spatial patterns of the total (HIST), thermodynamic (HIST – NAT), and dynamic (NAT) precipitation trends for the period 1980 – 2024. Basemaps are generated with cartopy.

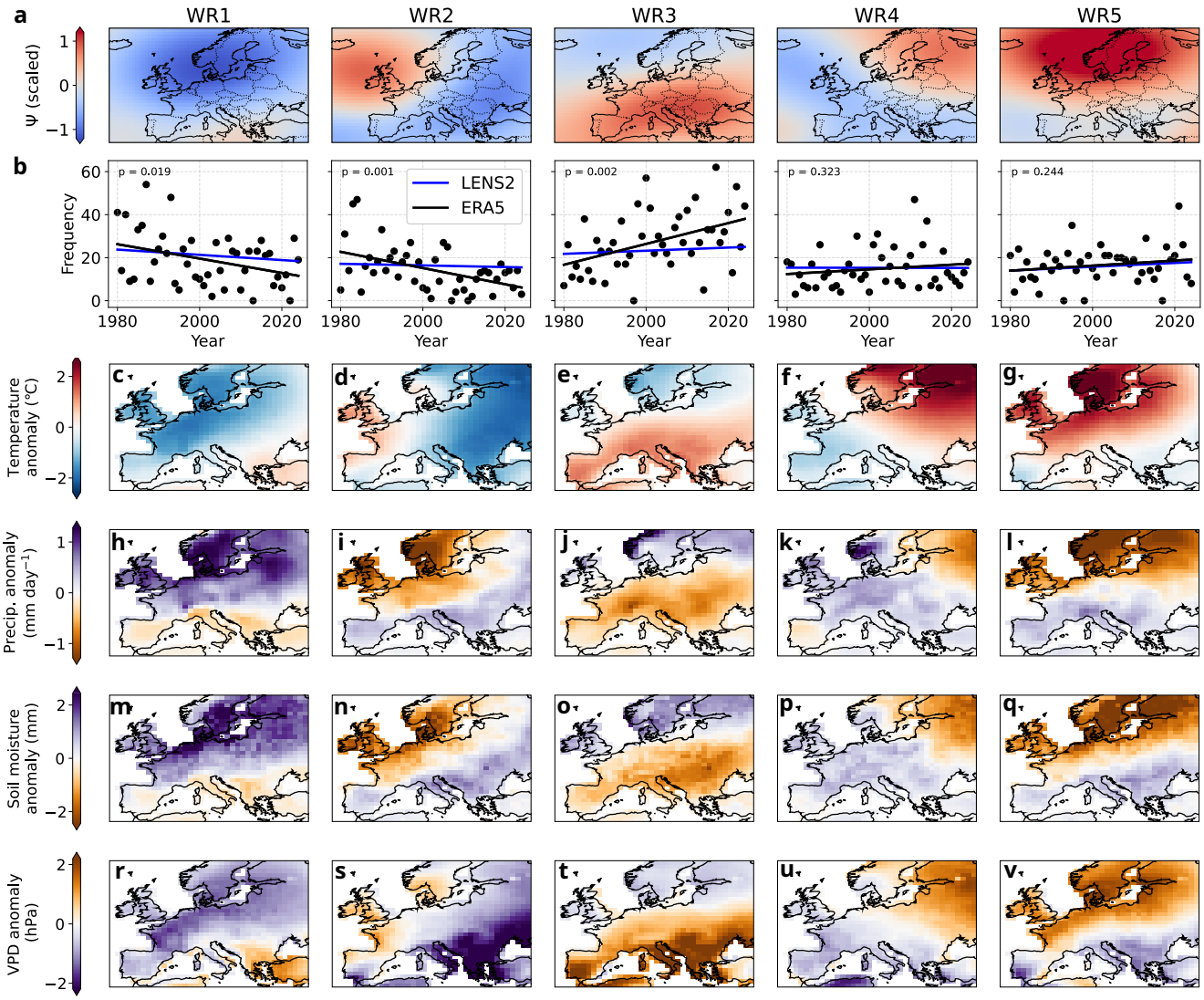

Supplementary Figure 4. Summertime weather regimes (WRs) and their imprint on European hydroclimate anomalies. a The 500 hPa streamfunction (Ψ) of five European summertime WRs, and b their trend in occurrence with blue lines for the mean trend across all LENS2 members. The p-values correspond to a two-sided t-test of the null hypothesis that the trends in ERA5 are zero. Mean anomaly of the present day simulations under each WR for temperature (c, d, e, f, g), precipitation (h, i, j, k, l), 10 cm soil moisture (m, n, o, p, q), and vapour pressure deficit (VPD) (r, s, t, u, v). Basemaps are generated with cartopy.

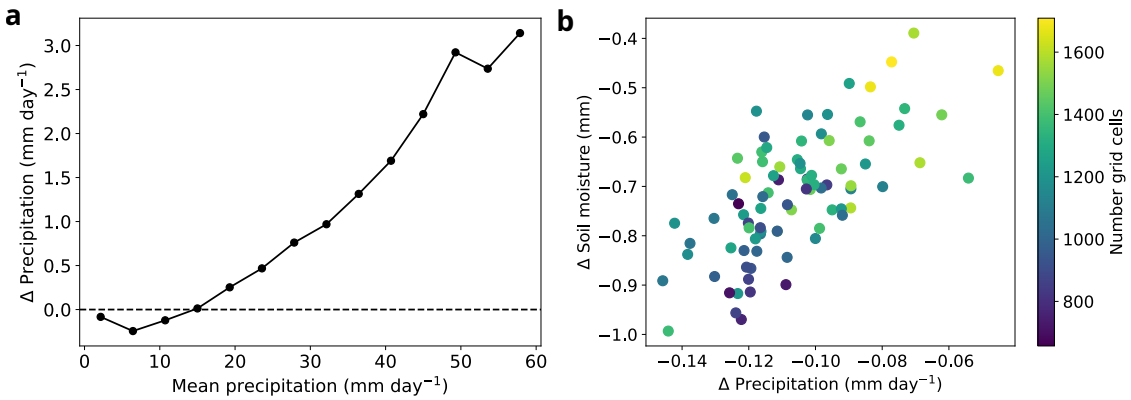

Supplementary Figure 5. Intensification of precipitation anomalies under thermodynamic forcing. a Relationship between daily precipitation event size and Δprecipitation (present day – natural forcing). Daily precipitation data is pooled and binned over the whole domain, then the mean of daily Δprecipitation is calculated for each bin. b Variations in seasonal mean Δsoil moisture are explained by seasonal mean Δprecipitation. Colors show the number of grid cells with days of more than 15 mm of precipitation. This reveals that Δsoil moisture is explained by Δprecipitation, and Δprecipitation by precipitation event size. All data for summer months.

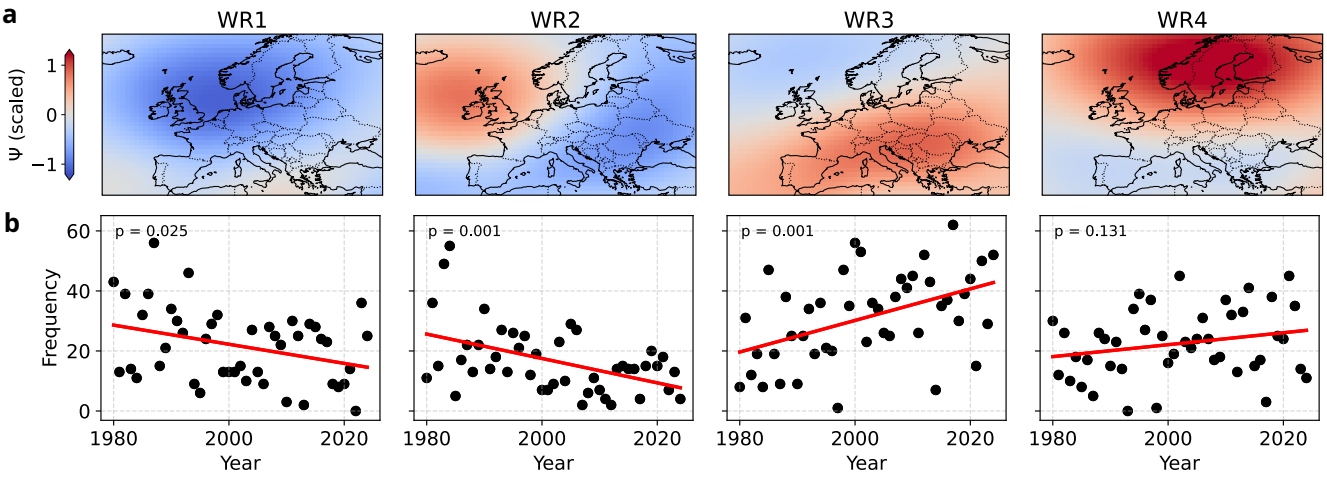

Supplementary Figure 6. Summertime weather regimes (WRs) with four clusters. a The 500 hPa streamfunction (Ψ) of four European summertime WRs, and b their trend in occurrence. The p-values correspond to a two-sided t-test of the null hypothesis that the trends in ERA5 are zero. Basemaps are generated with cartopy.

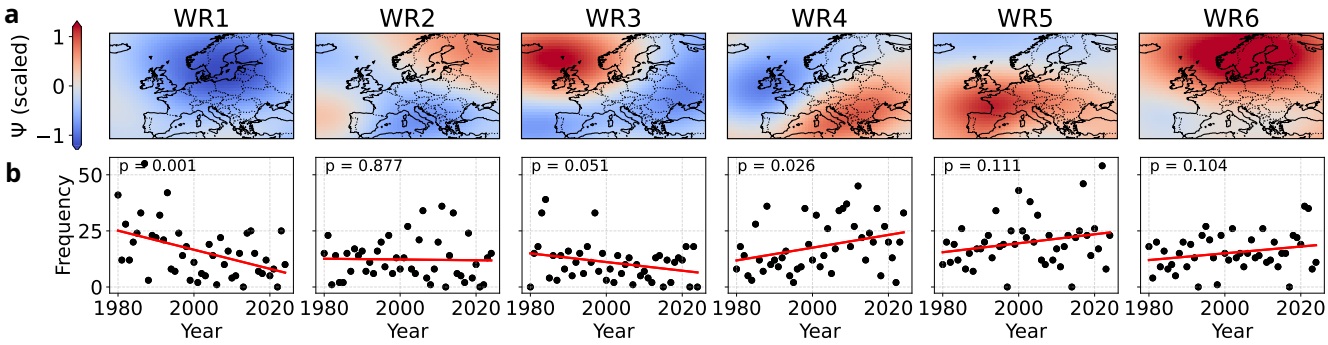

Supplementary Figure 7. Summertime weather regimes (WRs) with six clusters. a The 500 hPa streamfunction (Ψ) of six European summertime WRs, and b their trend in occurrence. The p-values correspond to a two-sided t-test of the null hypothesis that the trends in ERA5 are zero. Basemaps are generated with cartopy.